IEEE Access
Multidisciplinary ⋮ Rapid Review ⋮ Open Access Journal

Received 18 February 2023, accepted 4 April 2023, date of publication 12 April 2023, date of current version 4 May 2023.

Digital Object Identifier 10.1109/ACCESS.2023.3266654

RESEARCH ARTICLE

Research on Push-Pull Energy Storage PWM Power Drive of High-Power High-Response Proportional Solenoid

YAN QIANG[1,2], DANDAN YANG[1], LIN WANG[1], ZHIHANG DU[1], AND LIEJIANG WEI[1]

[1]Energy and Power Engineering College, Lanzhou University of Technology, Qilihe, Lanzhou, Gansu 730050, China
[2]Key Laboratory of Energy Conversion and Process Measurement and Control Ministry of Education, School of Energy and Environment, Southeast University, Xuanwu, Nanjing, Jiangsu 210096, China

Corresponding author: Liejiang Wei (weiliejiang@126.com)

This work was supported by the National Key Research and Development Program of China under Grant 2020YFB2009800.

ABSTRACT As the traditional power drive circuit is difficult to meet the requests of high-power high-frequency proportional solenoid fast drive, this paper proposes a push-pull energy storage pulse width modulation (PWM) power drive circuit. The circuit is equipped with an energy storage module, which releases energy when the proportional solenoid coil is charged, supplements the output of the power supply current, and shortens the arrival time of the steady-state current. When the coil is discharged, it recovers energy and shortens the time for the coil current to return to zero. In this paper, a theoretical model of push-pull energy storage power drive circuit is established, and simulation analysis and experimental verification are carried out for a proportional solenoid coil with rated current of 3.3A and power of 79W. The results show that the push-pull storage PWM power drive has excellent input-output linearity, minimal ripple, and good steady-state current output performance. Compared with the traditional single switch and reverse discharging power drives, the coil charging speed under the push-pull energy storage type power drive is increased by 25%, and the discharge speed is increased by 95% and 45% respectively.

INDEX TERMS High power, high response, proportional solenoid, push-pull energy storage, power drive.

I. INTRODUCTION

To satisfy the application requirements of high performance electro-hydraulic proportional control system in which the power of industrial equipment is constantly increasing and the precision and response speed of the control system is constantly improving, the electro-hydraulic proportional valve is developing towards the direction of large flow, high-frequency response, and intelligent control [1]. The high-power high-frequency proportional solenoid is used as the electro-mechanical converter of large flow high-frequency response electro-hydraulic proportional control valve. Its working performance is an important factor affecting the dynamic characteristics of the proportional valve. Proportional solenoid controls current through power drive [2], research on proportional solenoid power drive is an important way to improve the performance of solenoids. To obtain favorable power drive characteristics for solenoids, strenuous efforts in structure innovation and control strategy optimization have been made by many scholars at home and abroad.

In aspect of control strategies, Amirante et al. proposed a PWM modulation technology, which uses a high duty cycle to drive the proportional valve at the initial stage of opening, and uses a low duty cycle to maintain the target position of the spool. This method speeds up the response speed of the electro-hydraulic proportional valve [3]. Wang et al. proposed a multi-objective optimization strategy based on genetic algorithm, and applied the high-precision measurement device to the static thrust test and dynamic DC input signal test, which improved the dynamic response of the drive [4]. For the solenoid driven by the PWM method, Jung et al. proposed a resistance estimation method to compensate the duty cycle

The associate editor coordinating the review of this manuscript and approving it for publication was Alexander Micallef.

of the PWM signal so that it is proportional to the solenoid current [5]. Lu et al. adopted a pre-energizing control strategy based on a dual power supply to speed up the opening response time of the high speed solenoid injectors [6]. Meng has carried out system modeling and coupling analysis with a proportional solenoid valve (PSV) controlled by PWM. The corresponding coupling analysis results have certain reference value for the performance design and optimization of PSV. For the proportional electromagnet control system, Oleg et al. proposed a state controller, which uses the coil inductance linearization and modal control principle to solve the problem of obtaining the dynamic characteristics required by the electromagnet motion system [7]. Lim et al. proposed a dual-rate cascade control method, combining a fast inner loop current controller and a slower PID outer loop trajectory controller to convert a switching solenoid into a proportional actuator [8]. Xu, Liu et al. have found that the control of the dithering current can effectively reduce the hysteresis effect of the solenoid valve [9], [10]. To reduce the influence of the nonlinearity such as dead zone and low force gain with a small current on the performance of the valve, Jin et al. proposed a differential control method, outputting differential signals to energize the two solenoids of the proportional valve at the same time. The frequency response of the proportional valve is improved by analyzing the force output of the two solenoids to find the operating point. Peng established a simplified mathematical model using the power bond graph, and carried out numerical analysis on the proportional solenoid by using Maxwell. Xiong et al proposed an incremental differential allocation strategy to coordinate the actions of two proportional solenoids driving a high-response proportional solenoid valve. To some extent, the bandwidth, transient response, and anti-interference ability of the solenoid valve are improved.

In terms of drive circuit, Jin et al proposed a drive circuit capable of dual-voltage supply and dual-stage current control, which shortens the response time of the solenoid valve [11], Lee et al. designed an electronic valve driving circuit with fast response characteristics by using a 3 power source. In experiments using a hydraulic system, the new circuit shortened the switching delay time from 5 ms to 1.55 ms [12]. Ye et al proposed a bi-state modulation scheme and designed the half-bridge power driving circuit to improve the current step response [13]. Kim et al designed the power saving circuit which can highly improve the efficiency by providing optimal current according to mechanical load [14]. The high voltage drive method proposed by Rexroth accelerates the current rising speed by increasing the bus voltage, but it has the risk of coil burning. Nie proposed a Tri-state modulation power drive circuit, which improves the dynamic performance of proportional solenoid to a certain extent by improving the modulation mode of PWM signal [15]. Zhang et al. developed a nonlinear mathematical model of the reverse unloaded power drive circuit and proposed a new current controller to eliminate the zero hysteresis phenomenon [16], [17]. A bilateral driving circuit was proposed by Liu et al., and its control

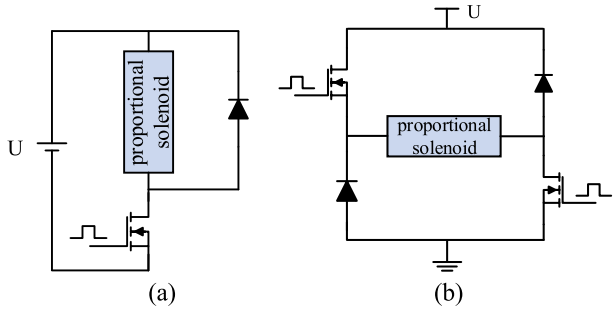

FIGURE 1. Conventional power drive circuit. (a) single switch power drive (b) reverse discharging power drive.

logic can avoid the current interruption, improve the positioning accuracy of the proportional spool [18], [19]. Currently, single switch drive circuit [20] and reverse discharging drive circuit [21] are the two most widely utilized drive circuits. Figures 1(a) and 1(b) show the two circuit structures, respectively. Although the single switch driven circuit has good stability and a wide range of duty cycle modification, current rises and falls slowly. When the coil is discharged, reverse discharging drive circuit switches the power supply voltage at both ends of the coil, which has a faster current decay speed, but the rising speed is not improved.

Due to the complexity and high use needs of intelligent algorithms, it has become crucial to focus on low-cost ways to enhance the driving circuit in order to increase the proportional solenoid's response time. The aforementioned drive circuits are used with low-current, low-power proportional solenoids, but they are still unable to meet the demands for high-power, proportional solenoid reaction speed in high-flow, high-frequency response proportional valves [22]. To maintain good steady performance of the proportional solenoid coil current while allowing the energy storage module to absorb energy when the coil is discharged to reduce the coil discharge time, this study offers a push-pull energy storage PWM power drive circuit. The push-pull energy storage PWM power drive circuit proposed in this paper combines the drive module and the energy storage module to ensure good steady performance of the proportional solenoid coil current while allowing the energy storage module to absorb energy during coil discharge to reduce coil dis-charge time and release energy during coil charging to reduce coil charging time to accelerate dynamic response.

The rest of the paper is organized as follows. Section II briefly introduces the principle and theoretical analysis of the push-pull energy storage PWM power drive circuit. Section III introduces the push-pull energy storage PWM power drive circuit's implementation methodology. In the Section IV, the circuit is simulated and analyzed, and the experiment results are carried out in Section V. Section VI presents some concluding remarks.

II. PUSH-PULL ENERGY STORAGE POWER DRIVE WORKING PRINCIPLE

To explore a power drive circuit suitable for high-power high-frequency loud proportional solenoid and accelerate the

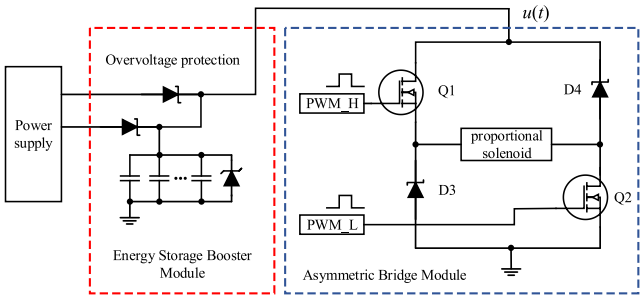

FIGURE 2. Schematic of Push-pull storage type PWM power drive main circuit.

dynamic response of proportional solenoid, this paper proposes a push-pull storage type PWM power drive. The main circuit structure of this power drive is shown in Fig2. Push-pull energy storage PWM power drive mainly consists of energy storage boost module and asymmetric bridge arm module. D1 and D2 are cur-rent-continuity diodes, and power tubes Q1 and Q2 are controlled by PWM signals for fast conduction and cutoff to realize the charging and discharging of proportional solenoid coils. The main circuit of the push-pull storage PWM power driver is divided into three states in the working process: the initial charging state, the ''pull-down'' state and the ''push-up'' state, and the simplified operating states of the main driver circuit are shown in Figure 3. A first-order ''L-R'' series model equivalent of the proportional solenoid is used in place of it, disregarding the solenoid's nonlinear inductance. L is the proportional solenoid equivalent inductance and R is the proportional solenoid equivalent resistance.

The PWM signal period is T, the duty cycle is D, and $0 \leqslant D \leqslant 1$. Relative to the R, the power tube and diode on resistance are very small, so the drive circuit charge and discharge state in the sum of these resistances are Rt, then the principle of each operating state is as follows.

A. INITIAL CHARGING STATE, t ∈ [0, DT]

Figure 3(a) depicts the push-pull storage power drive in its initial charging condition, with PWM H and PWM L high and power tubes Q1 and Q2 turned on and saturated by this control signal. The push-pull energy storage power drive now creates two charging circuits: a) the supply voltage U is delivered to the proportional solenoid coil via diode D1, power tubes Q1 and Q2, and b) the supply voltage U is charged to the energy storage capacitor C via diode D1. According to Kirchhoff's voltage law (KVL):

$$U = L\frac{di_s(t)}{dt} + (R + R_t)\, i_s(t) \tag{1}$$

In this condition, the proportional solenoid coil's current is

$$i_{on}(t) = \frac{U}{R + R_t}\left[1 - e^{\left(-\frac{t}{\tau}\right)}\right], \quad t \in [0, DT] \tag{2}$$

where: $i_s(t)$-proportional solenoid coil current; $i_{on}(t)$-proportional solenoid coil current in the initial charging state; τ-proportional solenoid time constant, and $\tau = L/R$.

B. "PULL DOWN" STATE, t ∈ [(k + D)T,(k + 1)T], k ∈ 0, 1, 2 . . .

Figure 3(b) illustrates a discharge circuit formed when the signal PWM H and PWM L are low, power tubes Q1 and Q2 cut off, a portion of the solenoid coil enters a discharge state, diodes D3 and D4 in the solenoid coil are subject to the effect of current continuity, creating a discharge circuit, the energy stored in the coil passes through the circuit into the energy storage capacitor C, causing the capacitor voltage u(t) to rise.

Since the energy stored in the coil is constant, there is formula (3):

$$W = Pt = \frac{u(t)^2 t}{R} \tag{3}$$

where, W- Proportional solenoid coil stored energy; P- The total power of the proportional solenoid unloading process; $u(t)$-Voltage applied across the proportional solenoid; t-Proportional solenoid coil discharge time.

According to the formula (3), when the voltage u(t) increases, the reverse pressure difference across the solenoid coil increases, and the time t will decrease, During this period, the coil current is rapidly ''pulled down'', shortening the discharge time of the proportional solenoid. At this time, the discharge circuit is equivalent to a second-order circuit, and the circuit equation in the ''lower'' state is obtained according to KVL:

$$-L\frac{di_s(t)}{dt} = (R + R_t)\, i_s(t) + u(t) \tag{4}$$

As a result, the proportional solenoid coil's current in the ''Pull-down'' state is

$$\begin{aligned} i_{off}(t) &= i_{off}(0)\, e^{-\alpha t}\cos(\omega_d t) \\ &\quad + \left(\frac{u(0) - \alpha L i_{off}(0)}{L\omega_d}\right) e^{-\alpha t}\sin(\omega_d t), \\ &\quad t \in [(k + D)T, (k + 1)T], \quad k \in 0, 1, 2\cdots \end{aligned} \tag{5}$$

where, $i_{off}(t)$-proportional solenoid coil current in the pull-down state;

$\alpha = \frac{(R+R_t)}{2L}$-attenuation factor of the discharge loop;

$\omega_d = \sqrt{\frac{1}{LC} - \left(\frac{R+R_t}{2L}\right)^2}$-the damped natural frequency of the discharge loop.

C. "PULL UP" STATE, t ∈ [kT, (k + D)T], k ∈, 1, 2, 3 . . .

State 3 is the non-initial charging state of proportional solenoid, ''push up'' state. At this time, PWM_H and PWM_L are high, power tube Q1, Q2 saturation conduction. During this time, the energy stored in the storage capacitor is first released and loaded onto the ends of the solenoid coil. This process continues until the voltage across the capacitor equals the power supply voltage U, at which point the coil is powered by U. Figure 3(c) depicts the loop created by this procedure. Through the combined action of the two loops, the

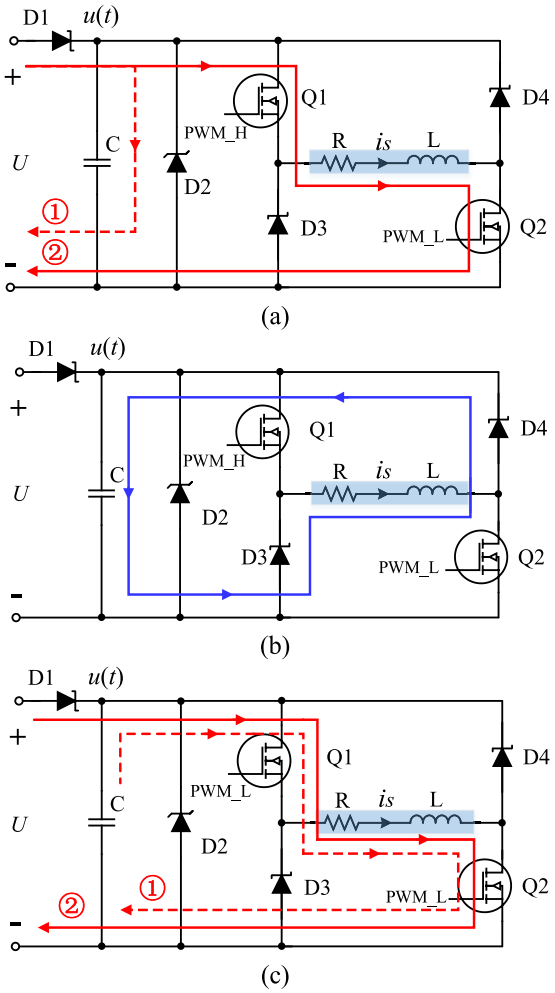

FIGURE 3. Working states. (a) Description of what is contained in the first panel; (b) Description of what is contained in the second panel. Figures should be placed in the main text near to the first time they are cited. A caption on a single line should be centered.

solenoid coil current is quickly pushed up to the steady state. The equation of loop 1 is obtained from KVL as

$$u(t) = (R + R_t)\, i_s(t) + L\frac{di_s(t)}{dt} \tag{6}$$

$$i_{on}(t) = i_L(kT)\, e^{-\alpha t}\cos(\omega_d t) + \left(\frac{u(kT) - \alpha L i_L(kT)}{L\omega_d}\right) e^{-\alpha t}\sin(\omega_d t)$$
$$t \in [kT, (k+D)T], \quad k \in N + 且 u(t) > U \tag{7}$$

where, i_L-the current on the equivalent inductance of the proportional solenoid; $i_{on}(t)$-proportional solenoid coil current in the initial charging state; $\alpha = \frac{(R+R_t)}{2L}$-attenuation factor of the discharge loop; $\omega_d = \sqrt{\frac{1}{LC} - \left(\frac{R+R_t}{2L}\right)^2}$-the damped natural frequency of the discharge loop.

Loop 2 equation is

$$U = L\frac{di_s(t)}{dt} + (R + R_t)\, i_s(t) \tag{8}$$

$$i_{on}(t) = \frac{U}{R+R_t}\left[1 - e^{(-\frac{t}{\tau})}\right], \quad t \in [kT, (k+D)T]$$
$$k \in 1, 2, 3\cdots, 且(t) \le U \tag{9}$$

Through the above analysis, it can be seen that the push-pull energy storage PWM power drive circuit in the process of operation, first after the initial charging state, and then in the state 2 and state 3 between each other, the use of energy storage capacitors to absorb and release the energy stored in the coil, to achieve the solenoid coil current quickly follow the given signal and complete the role of power drive.

According to the formula (4)-(7) can be known push-pull energy storage PWM power drive circuit under the step signal excitation, the coil charging and discharging speed is

$$\begin{cases} \left|\frac{di_{on}(t)}{dt}\right| = \left|\frac{1}{\tau}\frac{u(t)}{R+R_t}e^{-\frac{t}{\tau}}\right|, & \text{charge} \\ \left|\frac{di_{off}(t)}{dt}\right| = \left|-\frac{i_{off}(t) + \frac{u(t)}{R+R_t}}{\tau}e^{-\frac{t}{\tau}}\right|, & \text{discharge} \end{cases} \tag{10}$$

According to Figure 1(a), the response of the single-tube modulated power driver to the step signal can be expressed as

$$\begin{cases} L\frac{di_{ons}(t)}{dt} + i_{ons}(t)(R+R_t) = U, & \text{rising step} \\ L\frac{di_{offs}(t)}{dt} + i_{offs}(t)(R+R_t) = 0, & \text{descending step} \end{cases} \tag{11}$$

where i_{ons} – single switch charging state coil current; i_{offs} – single switch discharge state coil current.

Therefore, the charging and discharging speed of the proportional solenoid coil un-der single switch power drive is

$$\begin{cases} \left|\frac{di_{ons}(t)}{dt}\right| = \left|\frac{1}{\tau}\frac{U}{R+R_t}e^{-\frac{t}{\tau}}\right|, & \text{charge} \\ \left|\frac{di_{offs}(t)}{dt}\right| = \left|-\frac{i_{offs}(t)}{\tau}e^{-\frac{t}{\tau}}\right|, & \text{discharge} \end{cases} \tag{12}$$

According to Figure 1(b), the response of the reverse discharging power drive to the step signal can be expressed as

$$\begin{cases} L\frac{di_{onf}(t)}{dt} + i_{onf}(t)(R+R_t) = U, & \text{rising step} \\ L\frac{di_{offf}(t)}{dt} + i_{offf}(t)(R+R_t) = -U, & \text{desending step} \end{cases} \tag{13}$$

where, i_{onf} - reverse unload charging state coil current; i_{offf}- reverse unload discharging state coil current.

Therefore, the charging and discharging speed of the proportional solenoid coil un-der the reverse discharging power drive is

$$\begin{cases} \left|\frac{di_{onf}(t)}{dt}\right| = \left|\frac{1}{\tau}\frac{U}{R+R_t}e^{-\frac{t}{\tau}}\right|, & \text{charging} \\ \left|\frac{di_{offf}(t)}{dt}\right| = \left|-\frac{i_{offf}(t) + \frac{U}{R+R_t}}{\tau}e^{-\frac{t}{\tau}}\right|, & \text{discharging} \end{cases} \tag{14}$$

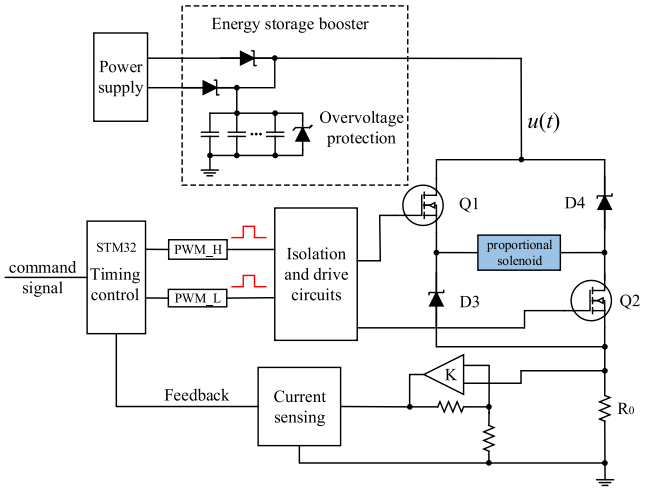

FIGURE 4. Push-pull energy storage type PWM power drive general structure.

The charging and discharging speed of the proportional solenoid coil under the three power drives is mainly related to the voltage loaded to the ends of the proportional solenoid coil when the time t is certain, the higher the voltage, the faster the charging and dis-charging speed of the coil, the setting of the energy storage module causes the voltage loaded to the ends of the proportional solenoid coil to rise, thus obtaining:

$$\begin{cases} \left|\frac{di_{on}(t)}{dt}\right| > \left|\frac{di_{ons}(t)}{dt}\right| = \left|\frac{di_{onf}(t)}{dt}\right|, & \text{charge} \\ \left|\frac{di_{off}(t)}{dt}\right| > \left|\frac{di_{offf}(t)}{dt}\right| > \left|\frac{di_{offs}(t)}{dt}\right|, & \text{discharge} \end{cases} \tag{15}$$

Equation (15) shows that, compared with the conventional power drive, the coil charging and discharging speed under the action of push-pull energy storage power drive is the fastest, which can accelerate the dynamic response of the proportional solenoid.

III. PUSH-PULL ENERGY STORAGE PWM POWER DRIVE IMPLEMENTATION

A controller module, a main circuit, an optocoupler isolation circuit, a gate drive circuit, an overvoltage protection circuit, and a current detecting feedback circuit comprise the push-pull energy storage PWM power drive. Figure 4 depicts the general structure of the power driver.

The main controller chip is STM32F103. After arithmetic processing, the main controller module turns the command signal and current feedback signal into PWM signal output and controls the coil current value by modifying the duty cycle of the PWM signal.

The primary circuit requires the power tube to saturate the conduction to ensure that the circuit can perform high-power drive. Because the push-pull energy storage power drive elevates the coil supply voltage in proportion to the solenoid coil charging process, increasing the difficulty of high-end tube conduction, the IR2110 gate driver chip was chosen for power tube Q1, Q2 drive. IR2110 with bootstrap

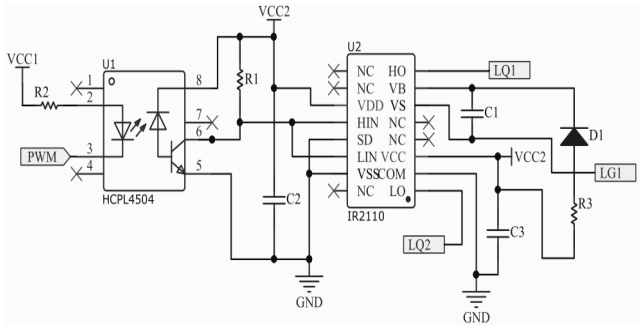

FIGURE 5. Isolated drive circuit.

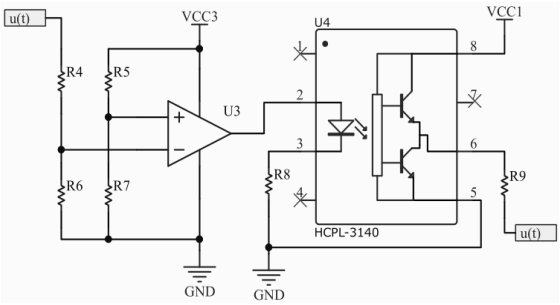

FIGURE 6. Overvoltage protection circuit.

capacitor to achieve regular high-voltage side MOS tube conduction. Simultaneously, the optocoupler isolation circuit is expanded to improve overall circuit security and anti-interference. Figure 5 depicts the isolated drive circuit of a push-pull storage PWM drive. LG1 is linked to the cathode of diode D3, while LQ1 and LQ2 are linked to the gates of power tubes Q1 and Q2, respectively.

The energy from the proportional solenoid coil is transmitted to the energy storage capacitor, causing the voltage of the energy storage capacitor to rapidly grow, and the overvoltage protection circuit is designed to prevent the capacitor from failing owing to the high voltage. The overvoltage protection circuit is shown in Figure 6. This section of the circuit is made up of a voltage comparison unit and a voltage drain unit, and the voltage divider circuit transmits the voltage on the energy storage capacitor to the voltage comparator's in-phase terminal for comparison with the threshold voltage.

Voltage comparator same-phase terminal voltage:

$$U_{1+} = \frac{R_2 V_r}{R_1 + R_2} \tag{16}$$

Threshold voltage:

$$U_{1-} = \frac{R_4 V_{CC\_2}}{R_3 + R_4} \tag{17}$$

When the capacitance voltage exceeds the threshold voltage, i.e. $U_{1+} > U_{1-}$, the comparator output voltage U_{out} is deflected, and the output high level causes the photocoupler secondary output to conduct with ground, and the excess capacitance voltage is re-leased to ground via resistor R9, thereby protecting the boost storage module's circuit.

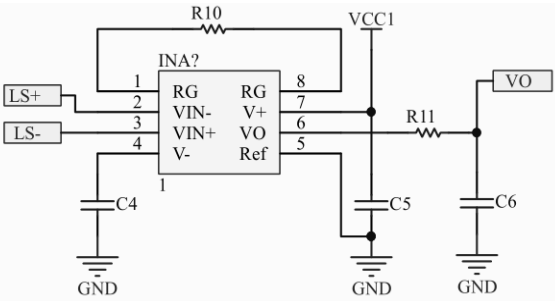

FIGURE 7. Current detection feedback circuit.

TABLE 1. Main parameters of power drive circuit.

Physical quantities	Parameter Value
Proportional Solenoid Equivalent Resistance R	4Ω
Power supply voltage U	+24V
Storage capacitor C1	120μF
Power MOS transistor on-resistance	0.09Ω
Zener diode conduction voltage drop	1V
Freewheel diode conduction voltage drop	0.7V

To provide real-time coil current collection and detection, the current sampling feed-back circuit employs a specific instrumentation amplifier INA128, which collects and amplifies the voltage difference on the sampling resistor R0 before sending it to the internal STM32 after ADC conversion. Figure 7 depicts the current detection circuit of the push-pull power driver. LS + and LS- are linked to the sampling resistor's two ends.

IV. PUSH-PULL ENERGY STORAGE POWER DRIVE SIMULATION STUDY

The main circuit model of the push-pull storage PWM power driver is built in the circuit simulation software LTspice, simulated and analyzed, and the main simulation parameters are shown in Table 1.

A. STEADY-STATE CURRENT CHARACTERISTICS

Figures 8(a) and 8(b) illustrate the simulated waveforms of the push-pull energy storage PWM power drive circuit's output steady-state current. The coil output currents corresponding to different PWM signal frequencies are basically the same under the same average voltage, indicating that the circuit has good linearity between input voltage and output current, and the higher the PWM signal frequency, the smaller the power drive circuit's turn duty cycle, and the duty cycle is proportional to the output current. Figure 8(c) shows the input and output characteristics of the three power drive circuits, push-pull energy storage, reverse discharging, and single switch, for the simulated case. All three power drive circuits exhibit good linearity characteristics, as shown in Figure 8(c). The duty ratio adjustment range of the push-pull energy storage and the reverse discharging drive circuit are similar, between 0.5-0.9, while the duty ratio adjustment

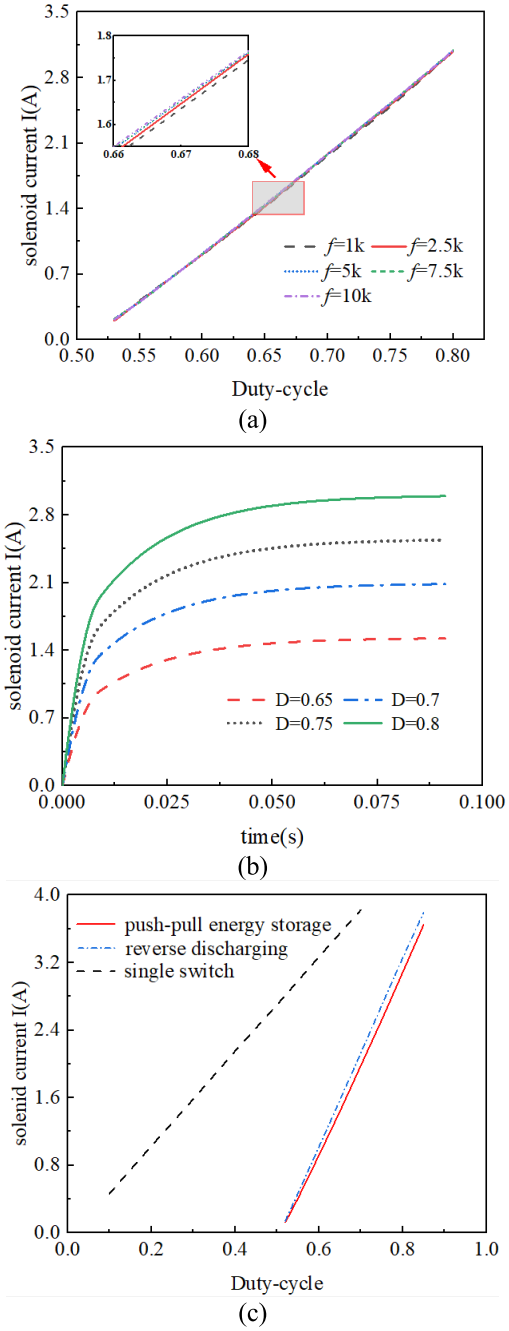

FIGURE 8. Working states. (a) Correspondence between coil current and duty cycle for different PWM signal frequencies; (b) Steady-state currents corresponding to different duty cycles of PWM signals; (c) Simulation curves of the input and output characteristics of the three power drivers.

range of the single-tube modulation drive circuit is between 0.1-0.7, but the current gain of the push-pull energy storage type and reverse connection unloading type drive circuit is large, which is more suitable for high-power conditioning applications.

B. DYNAMIC RESPONSE CHARACTERISTICS

The push-pull energy storage PWM power drive circuit is simulated with a rising step from 0 to 3.3A and a falling

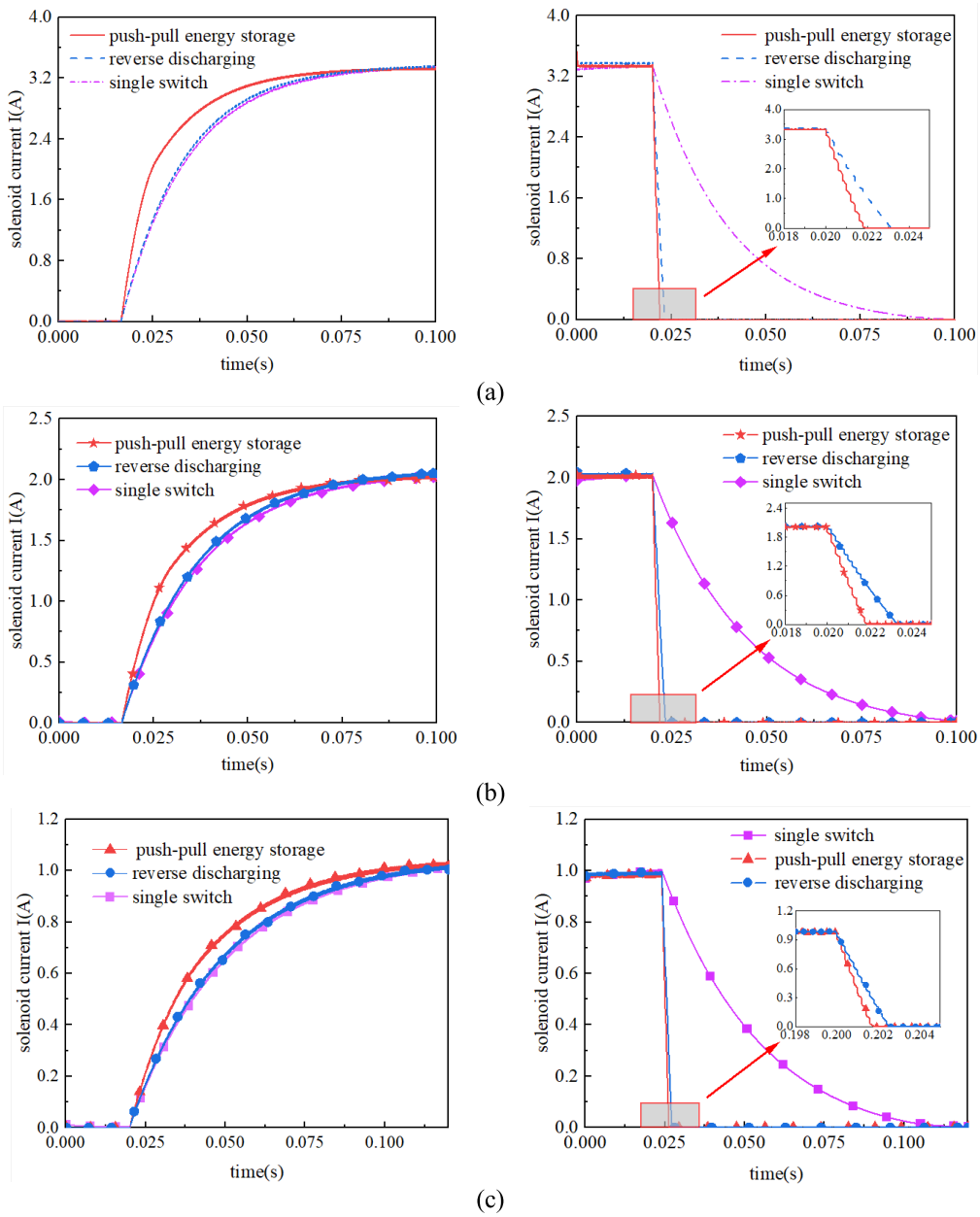

FIGURE 9. Step response simulation waveform. (a) Simulation waveforms of 0-3.3A rising and 3.3-0A falling step response of the three drives; (b) Simulation waveforms of 0-2A rising and 2-0A falling step response of the three drives; (c) Simulation waveforms of 0-1A rising and 1-0A falling step response of the three drives.

step from 3.3A to 0A, respectively, and compared with the single switch power drive and the reverse discharging power drive, and the simulation results are shown in Figure 9(a). The current rising speed of the push-pull energy storage drive circuit is the quickest in the rising step response, and the time necessary to climb to the steady-state current of the coil is the shortest, and the time for the current to increase to the steady-state value is 28.4ms. The current rise time output by the single switch and the reverse discharging drive circuit is almost the same, both are about 38ms, and the response time of the push-pull energy storage PWM power drive circuit is shortened by nearly 25%; the coil current decay speed of the single switch drive circuit is the slowest in the descending step response. When compared to a single switch, the current decay time is approximately 95% shorter, and it is around 46% shorter when compared to a reverse discharging power drive.

At the same time, the push-pull energy storage PWM power drive circuit is simulated for the rising and falling steps of 0-1A and 0∼2A, respectively. The simulation results are shown in Figure 9(b) and Figure 9(c) respectively. When compared to a single switch, the step response of the

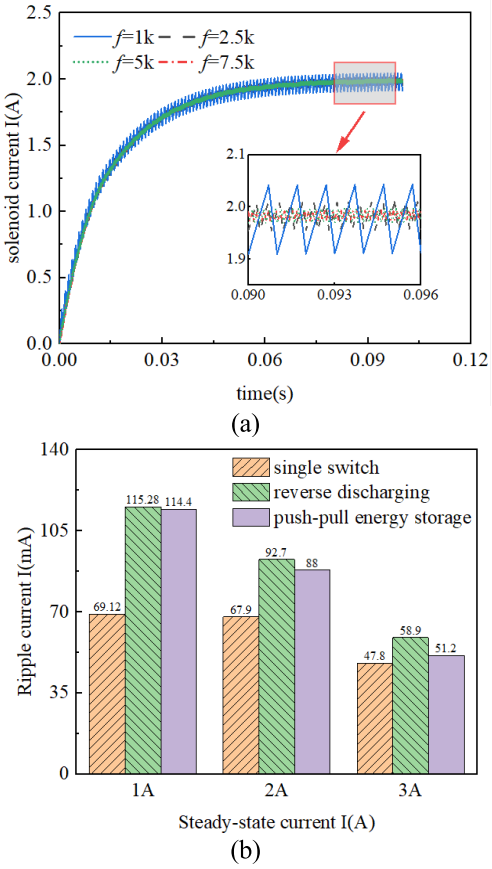

FIGURE 10. Ripple simulation curves. (a) Ripple curve with different PWM signal frequencies; (b) Three kinds of driving ripple comparison.

push-pull energy storage PWM power drive in the rising step of 0-2A is accelerated by 24%, and the step response of the falling step of 2-0A is accelerated by 96.5%, which is quicker than reverse discharging by 45%. The step response of the push-pull storage type PWM power drive is accelerated by around 22% in the rising step from 0 to 1A, and by 97.8% in the falling step from 1 to 0A when compared to the single switch and 44.5% when compared to reverse discharging.

As can be observed, the push-pull storage power drive circuit dramatically shortens the coil's charge and discharge time and speeds up the proportional solenoid's reaction.

C. RIPPLE

Because proportional solenoid ripple current consumes a lot of copper and iron, its energy conversion efficiency suffers, thus the power drive circuit output current ripple must be modest.

The output current simulation waveform of the push-pull energy storage power drive circuit at various PWM signal frequencies is shown in Figure 10(a). When the duty cycle of the drive circuit is fixed, the simulation waveform shows that the higher the PWM signal frequency, the smaller the output current ripple. This is because at the same time, the higher the frequency of the PWM signal, the smaller the step size of the current change, and the smaller the current jitter,

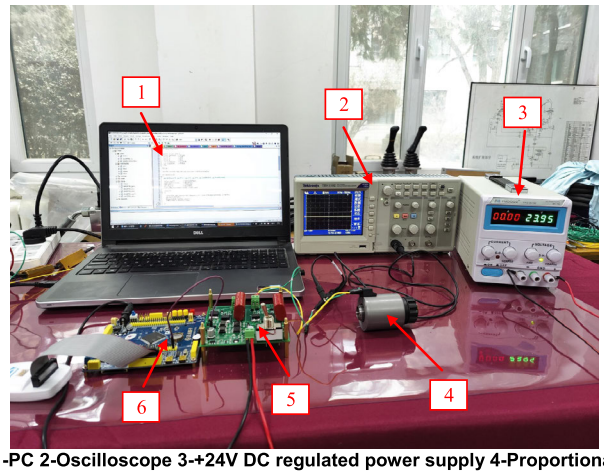

1-PC 2-Oscilloscope 3-+24V DC regulated power supply 4-Proportional solenoid 5-Power driver board 6-STM32 development board

FIGURE 11. Push-pull storage PWM power drive experimental platform.

so the smaller the ripple. When the current ripple of the three drive circuits at the same frequency is compared, it can be shown in Figure 10(b) that the ripple size of the three drive circuits steadily reduces with increasing steady-state current, with the reverse discharging drive circuit having the greatest ripple current. The current ripple of the push-pull energy storage drive is reduced to some amount when compared to the reverse discharging drive; the bigger the steady-state current, the less the output current ripple of the drive circuit. As the steady-state current increases, so does the push-pull. The ripple current of the energy storage type power drive circuit is the same as the ripple current of a single switch.

V. EXPERIMENTAL VERIFICATION OF PUSH-PULL ENERGY STORAGE POWER DRIVE

The performance of the push-pull energy storage PWM power drive circuit was validated by developing a power drive prototype, testing it on an experimental platform, and comparing it to the traditional power drive circuit. The solenoid for the GP63S threaded proportional valve is the control object. It has a rated current of 3.3A and a measured resistance of 4. Figure 11 depicts the push-pull storage type PWM power drive experimental platform, where the DC regulated power supply provides +24V supply voltage and the STM32F1 development board serves as the PWM signal output unit. During the experiment, the control algorithm converts the instruction signal into a PWM signal via the STM32F1 development board, and the power driver board amplifies the signal to drive the high-power proportional solenoid. To get the coil current signal, a 250mΩ sampling resistor is connected in series with the proportional solenoid, and the input and output signals of each module of the driver circuit are caught and shown by an oscilloscope.

A. EXPERIMENTAL STUDY OF STEADY-STATE CURRENT CHARACTERISTICS

The supply voltage is set to +24V, the frequency of the PWM signal is set to f=5kHz, and the duty cycle of the PWM signal

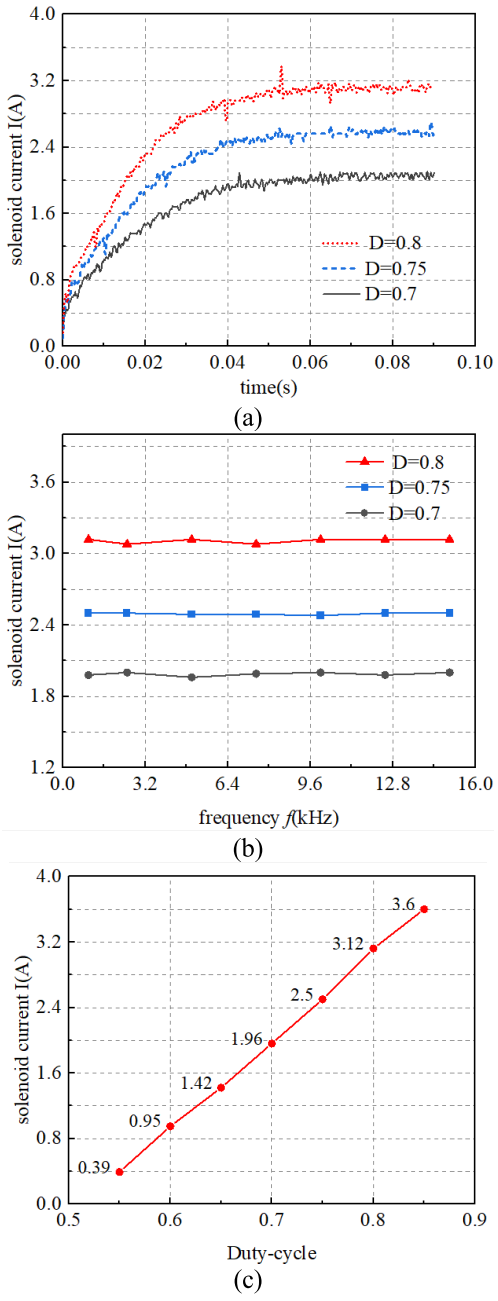

FIGURE 12. Push-pull storage PWM power drive experimental platform. (a) PWM signals with different duty cycle corresponding to steady-state current; (b) Steady-state currents corresponding to different PWM signal frequencies; (c) Push-pull power drive input PWM duty cycle vs. output current characteristic curve.

to 0.7, 0.75, and 0.8 respectively, and the corresponding steady-state current output curve is shown in Figure 12(a). It can be seen from the Figure 12(a) that the duty cycle of the PWM signal determines the average voltage applied to the proportional electromagnet. The larger the duty cycle, the higher the average voltage applied to the electromagnet coil, and the greater the output current of the power driver. Set the duty cycle of the PWM signal to 0.7, 0.75, 0.8, and record the steady-state current values at 1kHz, 2.5kHz, 5kHz, 7.5kHz, 10kHz, 12.5kHz, and 15kHz, respectively, to obtain the experimental results shown in Figure 12(b). Under the same duty cycle, when the PWM signal frequency varies, the current value of the power drive circuit output is nearly constant, and the drive circuit output is more stable.

PWM signal frequency to maintain f = 5kHz, set the duty cycle of the PWM signal step for 0.5 and increase one by one, record the steady-state value of the proportional solenoid coil current, the input and output characteristics of the push-pull energy storage PWM power drive circuit is shown in Figure12(c), it can be seen that the input and output of the push-pull energy storage PWM power drive circuit is approximately proportional, linearity is more obvious. A least squares fit is performed to obtain a functional relationship between the PWM control signal duty cycle D and the output current I:

$$I = 10.75D - 5.53 \tag{18}$$

Further, a functional relationship between the input voltage and the output current is obtained as follows:

$$I = 0.448U - 5.534 \tag{19}$$

The maximum current error of the push-pull storage type PWM power drive circuit is calculated to be 0.052A, and the linearity error is:

$$\frac{0.052}{3.6 - 0.39} \times 100\% = 1.6\% \tag{20}$$

The above analysis of the experimental findings shows that the linearity error of the drive circuit is 1.6%, and the maximum steady-state current output can reach 3.6A. The push-pull energy storage PWM power drive circuit has good steady-state current output performance and sufficient power driving capability.

B. EXPERIMENTAL STUDY OF STEP RESPONSE CHARACTERISTICS

The experimental waveforms of the rising and falling step responses of the output current of the push-pull energy storage, reverse discharging, and single switch power drive are shown in Figure 13(a).

The test settings remain unchanged: the peak PWM control signal is 3.3V with a frequency of 5kHz. The experimental rise and fall step waveforms show that the rise step time (rise to 90% of the steady-state current) of the single switch and reverse discharging power drive circuits are nearly equal, both being 39.4ms, whereas the rise time of the push-pull energy storage power drive circuit is 29.9ms, which is 24% shorter than the current rise time. The fall step time of the single switch drive is 40.5ms, the fall time of the reverse discharging drive is 4ms, and the fall time of the push-pull energy storage drive is 2.2ms. The fall step response time of the push-pull energy storage PWM power drive is 94.6% shorter than that of the single switch drive, and 45% shorter than that of the reverse discharging drive.

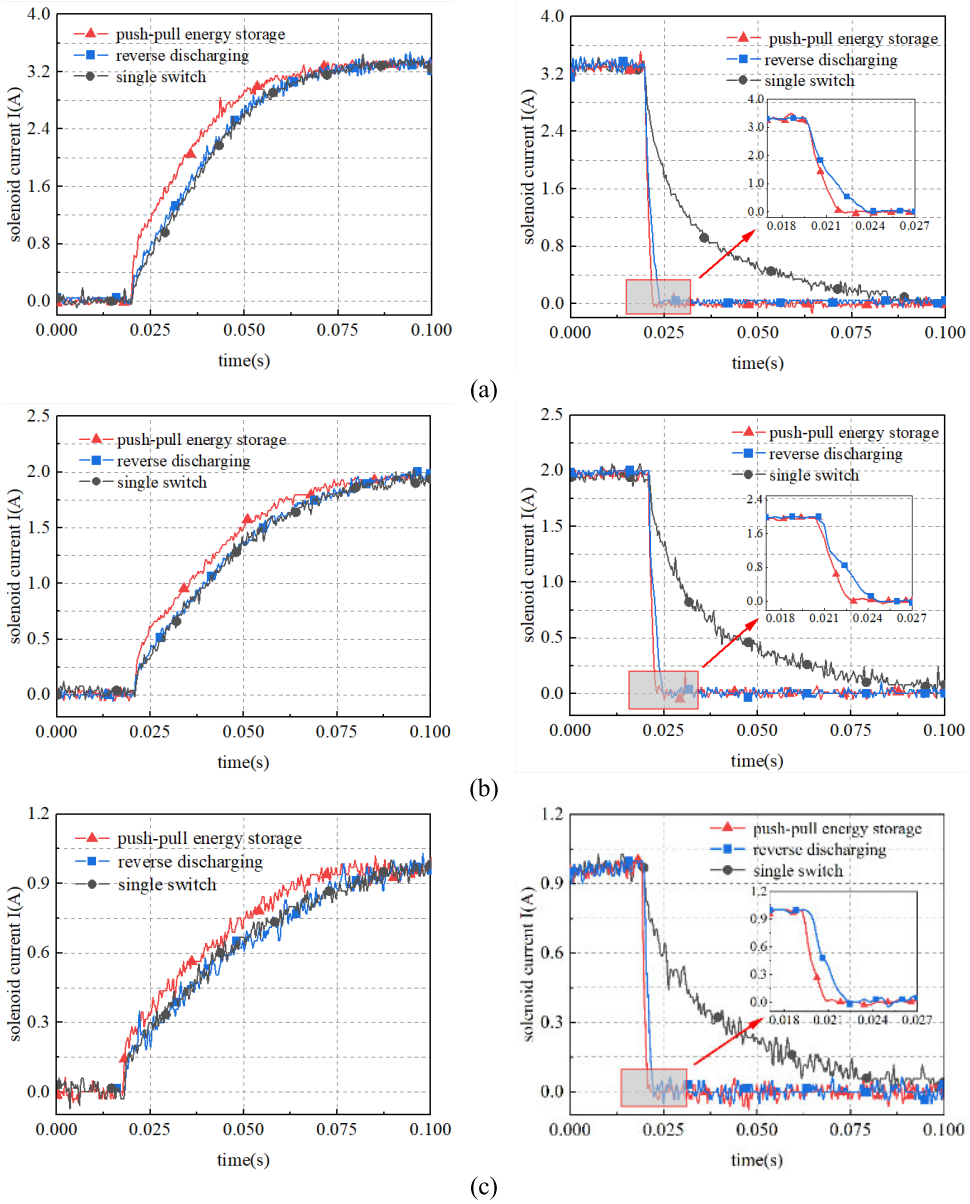

FIGURE 13. Step response experimental waveforms. (a) Experimental waveforms of 0-3.3A rising and 3.3-0A falling step response for the three drives; (b) Experimental waveforms of 0-2A rising and 2-0A falling step response for the three drives; (c) Experimental waveforms of 0-1A rising and 1-0A falling step response for the three drives.

TABLE 2. Comparison of simulation and experimental results of upward step response.

Steady-state current	rise step	Push-pull energy storage relative to single switch percentage reduction	Push-pull energy storage relative to reverse discharging percentage reduction
1A	Simulation	22%	22%
	experiment	21.2%	20.8%
	error	0.8%	1.2%
2A	simulation	24%	24%
	experiment	23.1%	23%
	error	0.9%	1%
3.3A	simulation	25.3%	25.3%
	experiment	24.5%	24.1%
	error	0.8%	1.2%

The experimental waveforms of the rising step and falling step responses of 2-0A for the output current of 0-2A for the three power drive circuits are shown in Figure 13(b). The rise step time of both the single switch and reverse

TABLE 3. Comparison of simulation and experimental results of descending step response.

Steady-state current	descending step	Push-pull energy storage relative to single switch percentage reduction	Push-pull energy storage relative to single switch percentage reduction
1A	Simulation	97.8%	44.5%
	experiment	97.4%	43.7%
	error	0.4%	0.8%
2A	simulation	96.5%	45%
	experiment	96.1%	43.8%
	error	0.4%	1.2%
3.3A	simulation	95.1%	45.7%
	experiment	94.6%	45.0%
	error	0.5%	0.7%

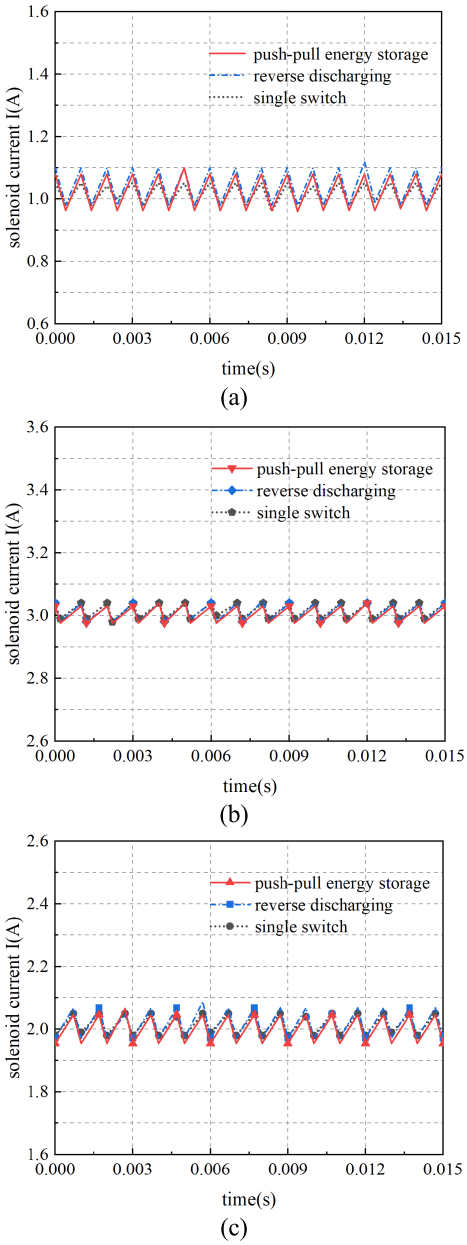

FIGURE 14. Experimental waveforms of output current ripple of three power drives. (a) Ripple at average current 1A; (b) Ripple at average current 2A; (c) Ripple at average current 3A.

discharging power drives is roughly 47ms, whereas the rise time of the push-pull storage power drive is 36.2ms, resulting in a 23% reduction in current rise time. The falling step reaction times of the three power drives are 1.8ms, 3.2ms, and 47.3ms, respectively, and the falling step response time of the push-pull energy storage type power drive circuit is accelerated by 96.1% and 43.8%, respectively. Fig 13(c) shows the experimental waveforms of the rising step and 1-0A falling step response of the three power driving output currents of 0-1A respectively. The rising step response time of the single switch drive circuit is 57.2ms, and the falling step response time is 57ms; the rising step response time of the reverse discharging is 56.9ms, and the falling step response time is 2.66ms. The current rising time of the push-pull energy storage power drive is approximately 21% shorter than the first two, and the falling time is 97.4% and 43.7% shorter respectively.

The simulation results are compared with the experimental results, and the results are shown in Tables 2 and 3. Due to the limitation of the experimental environment, there is a certain error between the experimental results and the simulation results, but the simulation of the step response time of the three power drive circuits is basically consistent with the experimental results. Combining the proportional solenoid's step response curve with tables 2 and 3, it can be shown that the greater the rising step load current, the better the effect of the push-pull energy storage drive circuit, and the lower step the lower the load current, the better the effect of the drive circuit. Under all operating situations, the charging and discharging speed of the proportional solenoid coil is significantly in-creased. The step response testing results show that the push-pull energy storage PWM power drive circuit considerably accelerates the step response of the proportional solenoid and reduces the step response time by nearly the same amount as traditional power drives.

C. EXPERIMENTAL STUDY OF RIPPLE

Figure 14 depicts the ripple experimental findings for three power drives with a 3.3V PWM signal peak, a frequency of 1kHz, and average output current values of 1A, 2A, and 3A, respectively. According to Figure 14, under the test conditions of this research, the ripples of the three power drive circuits steadily reduce as the steady-state current increases. The ripple of the push-pull energy storage power drive circuit is around 53mA when the steady-state current is 3A, while the ripple of the single switch is 50mA. The reverse dis-charging

power driver circuit has the highest ripple, about 60mA. The experimental findings are largely congruent with the simulation findings.

VI. CONCLUSION

This study presents a push-pull energy storage PWM power drive circuit for a high-power, high-response proportional solenoid, defines the power drive's working principle, and describes the specific hardware implementation. Experiment results show that:

1. When the solenoid coil requires fast charging, the energy storage module releases energy to supplement the current output of the power supply; when the coil requires fast discharging, the module absorbs energy, effectively speeding up the dynamic response of the high-power high-frequency loud proportional solenoid while ensuring steady-state performance.

2. The energy storage module recovers the coil energy of the proportional solenoid and uses it again for driving the proportional solenoid, realizing the secondary utilization of energy.

3. Push-pull energy storage PWM power drive with good steady-state current output performance, high input-output linearity, maximum non-linearity error of 1.6%, and sufficient power drive capability.

4. Under various operating situations, the step response properties of the proportional solenoid are greatly enhanced. The greater the load current in the rising step, the more the influence of the push-pull energy storage driving circuit; conversely, the lesser the load current in the falling step, the greater the effect of the driving circuit. When the steady-state current is 3.3A for a high-power proportional solenoid, the discharge time of the push-pull energy storage driving circuit is reduced by 94.6% compared to the single switch power drive and 45% compared to the reverse discharging power drive in the falling step response, and the coil charging time is reduced by 24% compared to the former two in the rising step response.

5. The ripple of push-pull energy storage type power drive gradually decreases with the increase of steady-state current, and compared with the reverse discharging drive, the ripple of push-pull energy storage type drive current is reduced to some extent; the larger the steady-state current, the smaller the ripple of the drive circuit output current, when the steady-state current continues to increase, the ripple current of the push-pull energy storage type power drive circuit is comparable to that of the single switch power drive.

It can be seen from the research that the charging and discharging time of the solenoid coil has been squeezed as much as possible. In order to further enhance the dynamic response of the high-power, high-response proportional solenoid, the control strategy optimization work is underway in our laboratory.

REFERENCES

[1] R. Han, "Analysis and design verification of switching loss and noise of high performance motor driver," M.S. thesis, Dept. Elect. China, Chong Qing Univ., Chong Qing, China, 2020.

[2] Y. Tominari and Y. Sato, "Three-phase AC linear proportional solenoid actuator with zero hysteresis in current–thrust force characteristics," *IEEE Trans. Magn.*, vol. 55, no. 7, pp. 1–8, Jul. 2019.

[3] R. Amirante, A. Innone, and L. A. Catalano, "Boosted PWM open loop control of hydraulic proportional valves," *Energy Convers. Manage.*, vol. 49, no. 8, pp. 2225–2236, Aug. 2008.

[4] S. Wang, Z. Wing, and B. Jin, "A performance improvement strategy for solenoid electromagnetic actuator in servo proportional valve," *Appl. Sci.*, vol. 10, no. 12, pp. 1–19, Aug. 2008.

[5] H. G. Jung, J. Y. Hwang, P. J. Yoon, and J. H. Kim, "Resistance estimation of a PWM-driven solenoid," *Int. J. Automot. Technol.*, vol. 8, no. 2, pp. 249–258, Feb. 2007.

[6] H. Lu, J. Deng, Z. Hu, Z. Wu, and L. Li, "Impact of control methods on dynamic characteristic of high speed solenoid injectors," *SAE Int. J. Engines*, vol. 7, no. 3, pp. 1155–1164, Apr. 2014.

[7] B. Oleg and T. Marina, "Regulator synthesis for the proportional electromagnet control system," in *Proc. Int. Conf. Ind. Eng., Appl. Manuf. (ICIEAM)*, May 2022, pp. 610–614. [Online]. Available: https://ieeexplore.ieee.org/abstract/document/9787185

[8] K. W. Lim, N. C. Cheung, and M. F. Rahman, "Proportional control of a solenoid actuator," in *Proc. 20th Annu. Conf. IEEE Ind. Electron.*, Sep. 1994, pp. 2045–2050. [Online]. Available: https://ieeexplore.ieee.org/abstract/document/398134

[9] Q. Xu, G. Wei, and X. Li, "Characteristic analysis and control for high speed proportional solenoid valve," in *Proc. IEEE 8th Conf. Ind. Electron. Appl. (ICIEA)*, Jun. 2013, pp. 1578–1582. [Online]. Available: https://ieeexplore.ieee.org/abstract/document/6566620

[10] G. Liu, W. Xia, D. Qi, and R. Hu, "Analysis of dither in PWM control on electro-hydraulic proportional valve," *TELKOMNIKA Indonesian J. Electr. Eng.*, vol. 11, no. 11, pp. 6808–6814, Nov. 2013.

[11] L. Jin, K. Zhang, Z. Qi, and M. Yang, "Solenoid valve driving module design for electronic diesel injection system," in *Proc. SAE World Congr. Exhib.*, Apr. 2005, pp. 4–8. [Online]. Available: https://www.researchgate.net/publication/293816972

[12] I.-Y. Lee, "Switching response improvement of a high speed on/off solenoid valve by using a 3 power source type valve driving circuit," in *Proc. IEEE Int. Conf. Ind. Technol.*, Dec. 2006, pp. 1823–1828. [Online]. Available: https://ieeexplore.ieee.org/abstract/document/4237833

[13] F. Ye, H. Chen, T. Gang, and Y. Liu, "Bi-state modulation for high speed on/off solenoid valve," *Adv. Electr. Eng. Electr. Mach.*, vol. 134, pp. 115–122, Jan. 2012.

[14] M. S. Kim and D. S. Kim, "A study of on/off solenoid actuator with power saving circuit," in *Proc. JFPS Int. Symp. Fluid Power*, Sep. 2008, pp. 477–482.

[15] Y. Nie and Q. Wang, "Tri-state modulation power driving of electro-hydraulic proportional amplifier," *Chin. J. Mech. Eng.*, vol. 22, pp. 639–644, Oct. 2009.

[16] J. Zhang, Z. Lu, B. Xu, Q. Su, D. Wang, and P. Min, "Investigation into the nonlinear characteristics of a high-speed drive circuit for a proportional solenoid controlled by a PWM signal," *IEEE Access*, vol. 6, pp. 61665–61676, 2018.

[17] B. Xu, Q. Su, J. Zhang, and Z. Lu, "Analysis for drive circuit and improved current controller for proportional amplifier," *J. Zhejiang Univ., Eng. Sci.*, vol. 47, pp. 2765–2778, Apr. 2017.

[18] N. Liu and Y. You, "Design of bilateral drive circuit on electro hydraulic proportional amplifier and comparison of dither signal," *J. Mech. Electr. Eng.*, vol. 37, no. 6, pp. 692–696, Jun. 2020.

[19] Q. Su, "Analysis and compensation methods for the pilot operated proportional directional valves," Ph.D. dissertation, Dept. Elect. China, ZheJiang Univ., ZheJiang, China, 2016.

[20] J. Zhang, D. Wang, B. Xu, Z. Lu, M. Gan, and Q. Su, "Modeling and experimental validation of the time delay in a pilot operated proportional directional valve," *IEEE Access*, vol. 6, pp. 30355–30369, 2018.

[21] W. Shi, J. Wei, J. Fang, and M. Li, "Nonlinear cascade control of high-response proportional solenoid valve based on an extended disturbance observer," *Proc. Inst. Mech. Eng., I, J. Syst. Control Eng.*, vol. 233, no. 8, pp. 921–934, Nov. 2018.

[22] T. Kramer and J. Weber, "Self-sensing position determination on a sensor-designed proportional solenoid," in *Proc. 12th Int. Fluid Power Conf.*, Jun. 2020, pp. 269–280. [Online]. Available: https://www.researchgate.net/publication/344659334

YAN QIANG was born, in February 1982. She received the Ph.D. degree in engineering. She is currently an Associate Professor and a Master Tutor. Her research interests include electro-hydraulic control system and fluid parameter measurement technology, fluid measurement, and the control in the field of medical-industrial combination. She was the project leader and participant in the National Key Research and Development Program, the National Natural Science Foundation of China, and other research projects.

DANDAN YANG received the B.S. degree in measurement and control technology and instrumentation and the M.S. degree in mechanical and electrical engineering from the College of Energy and Power Engineering, Lanzhou University of Technology, Lanzhou, China, in 2019 and 2022, respectively. Her research interest includes electro-hydraulic control technology.

LIN WANG received the B.S. degree in mechanical and electrical engineering from the School of Energy and Power Engineering, Lanzhou University of Technology, Lanzhou, China, in 2021, where she is currently pursuing the M.S. degree. Her research interest includes electro-hydraulic control systems.

ZHIHANG DU received the B.S. degree in measurement and control instrumentation and technology from the School of Energy and Power Engineering, Lanzhou University of Technology, Lanzhou, China, in 2021, where he is currently pursuing the M.S. degree. His research interest includes the development of valve controller based on embedded systems.

LIEJIANG WEI was born, in February 1972. He received the Graduate degree from the Lanzhou University of Technology, in 2009, and the Ph.D. degree in fluid machinery and engineering. He is currently a Professor and a Doctoral Supervisor with the Lanzhou University of Technology. His research interests include electro-hydraulic digital control systems and fluid parameter measurement technology. As the project leader, he is responsible for the National Key Research and Development Program ''Development of programmable digital controller for electro-hydraulic valves and systems with independent control of valve port'' and the National Natural Resources Foundation of China ''Research on a digital controller about the multiaxial electro-hydraulic dynamic loading system considering gap nonlinearity.'' Digital controller about the multiaxial electro-hydraulic dynamic-loading system in the non-linearity with backlash, ''Research on a digital controller about the multiaxial electro-hydraulic dynamic-loading system in the non-linearity with backlash ''Study on the electro-hydraulic load simulation system for the pitch control of mega-watt wind turbine with wide clearance nonlinearity wide clearance nonlinearity)'' and other scientific projects.